Proceedings of the ASME 2010 3rd Joint US-European Fluids Engineering Summer Meeting and 8th International Conference on Nanochannels, Microchannels, and Minichannels
FEDSM-ICNMM2010
August 1-5, 2010, Montreal, Canada

FEDSM-ICNMM2010-30977

CHARACTERIZATION OF SWITCHING TIME AND CELL STRESS IN A GRAVITY-DRIVEN MICROFLUIDIC CELL SORTER BASED ON HYDRODYNAMIC SWITCHING

Michael Grad
Columbia University
New York, NY, USA

Lubomir Smilenov
Columbia University
New York, NY, USA

David Brenner
Columbia University
New York, NY, USA

Daniel Attinger
Columbia University
New York, NY, USA

ABSTRACT

In this work we describe the control and characterization of the switching time and hydrodynamic stress in a microfluidic cell sorter. The device was designed to sort small (<1000) populations of live cells in buffer solution labeled with standard bio-markers such as live dyes or green fluorescent protein (GFP). Sorting occurs through a hydrodynamic switching technique where high-speed solenoid valves control a sheath flow used to steer sorted cells away from the unsorted bulk population. The device is constructed from a reusable hard plastic polymethyl-methacrylate (PMMA) chip machined with 127μm x 50μm microchannels and sealed with adhesive tape. Open reservoirs in the chip facilitate pipette access, standard microscope visualization, and a simple disassembly and cleaning procedure. The sorting frequency of this type of device is typically limited by the hydrodynamic switching time. Here, we present a theoretical and numerical analysis of the device switching time,. These results show that the sorter switching time t is practically limited by the velocity of the flow and the characteristic length between inlet and outlet channels. We validate this theoretical result with experimental data obtained from flow visualizations, along with experiments conducted to evaluate the repeatability of the hydrodynamic switching scheme and the survival rate of sorted fibroblast cells Manually operated, the sorting frequencies were approximately 10 cells per minute, with switching time constants of approximately 130ms. Current throughput is limited by this switching time to approximately 450 cells per minute. Automation can increase the velocity and reduce the spacing between cells, thereby increasing throughput by at least an order of magnitude. The cell sorter was then tested by manually sorting 100 beads in 7 minutes, and 30 cells in less than 3 minutes, and was successfully used in the framework of a study on the bystander effect occurring during cell irradiation. Experiments with Trypan Blue dye verified that cell viability was maintained during the sorting process.

1. INTRODUCTION

The sorting of single cells from larger cell populations has become a fundamental tool of biochemical research. Cell classification and sorting may be undertaken as a primary study objective or as a preparatory tool prior to subsequent assays. A broad range of analyses may rely on isolating subsets of cells from a heterogeneous population, including those related to molecular genetics, pathology diagnosis, etc. Typical cytometry applications deal with the analysis and sorting of >106 cells, however there is increasing interest in the sorting of smaller cell populations (10-100 cells). Investigations concerning single cell gene expression, miRNA profiling and DNA sequencing are considered extremely important sources of information reflecting most exact cell mechanisms [1, 2]. Also, extracellular interactions such as those found in the radiation-induced bystander effect may lead to a better understanding of the consequences of low-dose radiation [3]. In all of the above cases, large population-wide analysis may mask the behaviour of individual cells in biological processes where cellular heterogeneity plays a role [1]. Therefore there are many cases where single cells are separated from small populations and analyzed, and in such cases the capability of sorting $>10^6$ cells is unnecessary.

Several methods are currently available to sort single cells, and they differ with respect to the sorting mechanism, the

sorting efficiency, the sorting frequency, or the typical cell amount per batch. The most widely used device for cell sorting of large populations is the flow cytometer, based on Fluorescence Activated Cell Sorting (FACS). Commercially available products are available from companies such as Becton Dickinson, Coulter, Partec, and Union Biometrica, among others [4-6]. These commercial cytometers use either 'droplet deflection' or 'stream switching' to deflect cells into separate reservoirs. In the former case, cells are encapsulated into droplets, their fluorescence is measured, and they are electrostatically or pneumatically deflected into separate reservoirs. In the latter case, a piezoelectric fluidic valve deflects sorted cells. These products are mostly designed for fast separation of large populations, with typical throughputs ranging from 300 cells/second to over 10 000 cells/second [6]. Cells are typically fixed, and their application in the sorting of live cells may induce cell stress [7]. This requires subsequent cell recovery where the cell status before the sorting (frequently of great interest to the investigators) is lost. Also traditional flow cytometers are large, expensive instruments difficult to integrate into further processes involving microfluidic chips. Also, small populations of cells (~10-100) sorted in cytometers will be lost in the sample volume. Here we propose a microfluidic sorter meant to handle single cells from small populations, with the advantage of possible integration into other microfluidic processes.

Hydrodynamic cell sorters rely only on hydrodynamic forces to separate cells. A very simple example of an on-chip hydrodynamic cell sorter relies on flowing cells into a Y-connection and selectively blocking with e.g. a valve one outlet port so that cells are forced to the other outlet [13]. A drawback of this scheme is that cells such as fibroblasts might adhere to the channel walls when the flow is turned off. Also, turning off a valve may damage cells passing through it. For these two reasons, more sophisticated hydrodynamic cell sorters have been designed, with the goal to sort small amounts of cells with minimal losses. Hydrodynamic sorters that do not stop the outlet channel flow have been successfully shown in [14, 15]. Kruger et al. [15] described the development of a hydrodynamic cell sorter coupled with fluorescence detection. Sheath flow driven by syringe pumps was used to direct the flow from the main channel carrying beads to either one of two outlet channels. The flow was controlled by syringe pumps with a relatively long switching time, on the order of 200 milliseconds: this caused backpressure interferences and the authors concluded that their hydrodynamic switching device required more optimization in terms of precise flow control. Later, Dittrich et al. [14] used a X-shaped geometry analog to Kruger et al. [15] to sort cells, where electrokinetic forces drove the sheath flow.

This paper characterizes an optimized X-shaped hydrodynamic cell sorter where switching is driven by a sheath flow. Computational Fluid Dynamics is used to assess the performance of the device and the stress exerted on the cells. Channels are milled in a hard plastic. In our design, syringe pumps drive the sheath flow so that no electric forces are exerted on the cell. We use gravity to drive the main flow containing the cells, between open reservoirs that can be easily accessed by pipette. Also, fast solenoid valves with 0.5ms opening time are used to suppress backpressure interference, so that single cells can be individually sorted. Finally, the microfluidic channels are sealed with tape, which can easily be removed for cleaning the reusable chip.

2. CONCEPT AND DESIGN

Figure 1 shows the flow channel geometry of the cell sorter. The sorter involves the intersection of three inlet channels S1 (side inlet 1), S2 (side inlet 2), and I (cell inlet), and two outlet channels O1 (outlet 1) and O2 (outlet 2). Gravity drives a particle-laden solution from the inlet (I) to the intersection. At this point, cells are deflected to either outlet channel by a sheath flow determined by the state of two valves, located at S1 and S2, which are reciprocally open or closed.

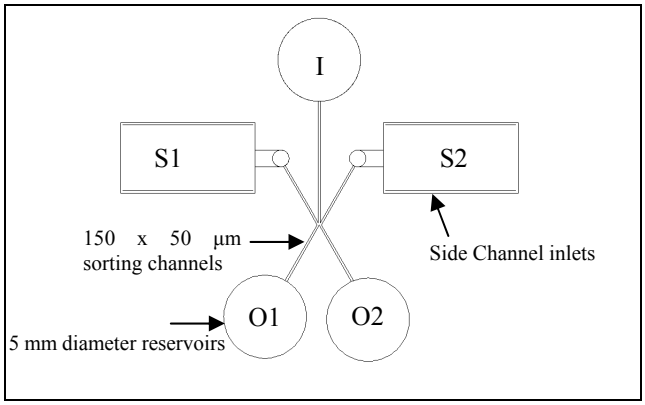

Figure 1: Schematic of cell sorter flow channels. The cells flow from I. Flows from S1 or S2 are used to deflect the cells into the outlets O1 or O2.

A hydrostatic pressure difference determined by a height difference Δh was created between the inlet and outlet reservoirs to drive the cell flow through the main channel, allowing free access with a pipette to the inlet and outlet reservoirs. To allow enough time for cell identification and sorting, the target design cell speed is chosen as V=0.5 mm/s, which corresponds to a visibility time of 2s for each incoming cell. The cross section of the channels was chosen to be 127 μm by 50 μm, about 10 times the cell size so that clogging is prevented, resulting in a hydraulic diameter D=72 μm. Assuming the cell solution has the volumic mass of water, ρ=1000 kg/m^3, and a viscosity of 0.001 Pa-s, we obtain a Reynolds number Re= $\rho UD/\mu$ of about 0.036. The flow is therefore clearly laminar with negligible inertial effects, and cells following streamlines without turbulent oscillations. The pressure difference ΔP between inlet and outlet reservoirs required to drive this flow is given by [16]:

$$\frac{64}{\mathrm{Re}}\frac{L}{D}\frac{1}{2}\rho V^2 = \Delta P = \rho g \Delta h \qquad \text{Eq 1}$$

For a travel length in the chip of L=20mm, we need a pressure difference ΔP=50 Pa, corresponding to a height difference between the reservoirs Δh=5 mm. The height of the inlet and outlet reservoirs are therefore designed to be at least 10 mm to give more control over the speed of the cells; this height is controlled by the overall thickness of the chip.

The side channel flows can also be provided by gravity flow, and this scenario was tested. It was decided to use a syringe pump, however, because one was available in our lab and because it allows an easy way to specify certain flow rates instead of specifying height differences. Gravity flow is recommended in labs where a syringe pump is not immediately available.

The target flow speed was chosen as 0.5 mm/s because this speed is slow enough for manual operation (taking into account human reflexes), and fast enough to prevent cells from adhering to the walls. A possible explanation for cells not adhering to the walls can come from the analysis of the Peclet number, Pe= LV/D, which is the ratio of convection to diffusion. In this equation, D, the diffusion coefficient defined by $K_BT/6\pi\eta r$ (Einstein) is approximately 1e-14, the velocity V is estimated at 0.5mm/s, and L is taken as 20 μm (half channel height). The Peclet number in our application is calculated to be 10^6. The large Peclet number means convection dominates, and particles do not diffuse to the walls for adhesion.

In the design process, we used Computational Fluid Dynamics to determine the and the maximum shear rate experienced by the cells. The finite-element multiphysics software COMSOL was used to simulate the flow at the intersection of three inlet channels and two outlet channels. A 3D mesh was generated by COMSOL with 10 nodes along the z-axis and 200 nodes along the x and y axes, corresponding to XY tetrahedral elements. As a boundary condition, a pressure difference of 50 Pa, corresponding to the above calculation from equation 1, was applied between the inlet and outlet reservoirs. The closed valve was modeled as a wall.

Figure 2 shows the outcome of a steady state flow simulation. In the configuration described, the top left valve is closed while the top right valve is open. The average speed of the flow in the simulation is about 0.8mm/s, in good agreement with the design goal of 0.5mm/s. Trajectories shown in black lines in Figure 2a show that the presence of a sheath flow at the right deflects the particle-laden flow towards the left channel. Reciprocally, figure 2b shows that in the opposite valve configuration deflects the particle-laden flow towards the right channel.

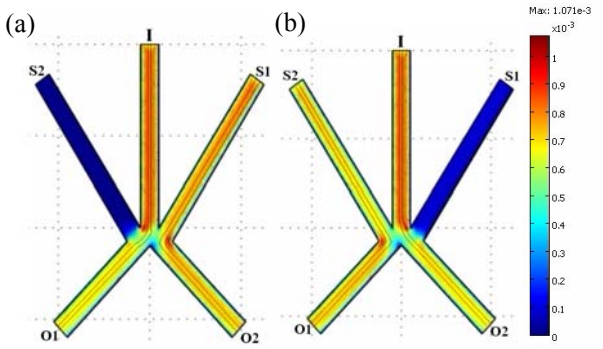

Figure 2: COMSOL simulation showing the velocity magnitude and streamlines for the two configurations, deflecting the inlet flow to the left and right depending on the state of the side inlets.

The switching time is dependent on two parameters: the time it takes to accelerate or stop by changing the pressure boundary condition the flow, and the time it takes to redirect the flow from the old outlet to the new outlet. Hydrodynamic theory predicts that the acceleration time depends on the diffusion of the fluid momentum across the channel. This can be expressed as [17]

$$t_{accel} = \frac{\rho}{\gamma_1^2}\frac{a^2}{\mu} = 0.97ms \qquad \textbf{Eq 2}$$

In the above equation, the symbols a, γ_1, μ, respectively stand for the hydraulic diameter, the smallest Bessel function root (γ_1 = 2.405), and the viscosity of the fluid. The time it takes to redirect the flow to the new outlet depends on the velocity and geometry of the channels. It is defined as the time it takes for a particle to cross the characteristic distance between one inlet channel and the opposite outlet channel. For the channel of cross sectional area A_{cs} = $6.35\cdot10^{-9}$ m^2, a switching flow rate Q_{sf} = 1 μl/min, and a characteristic length l = 300 μm,

$$\tau_{redirect} = \frac{A_{cs}l}{Q} = 114ms \qquad \textbf{Eq 3}$$

From the above analysis, it is shown that the acceleration switching time is smaller than the redirection switching time. An experiment with blue dye flowing from the input and pure water flowing from the side channels was performed to validate this switching time calculation. The valves were connected to a function generator and operated to send the flow in alternating directions at varying frequencies. A high-speed camera was used to image the flow and study the switching time (figure 3). The movie shows that it takes approximately 133ms to switch the flow from one channel to the other. This corresponds to a maximum throughput of approximately ~450 cells per minute, at a flow rate of 1 μl / min. This throughput can be increased with higher velocities, as discussed in section 5.

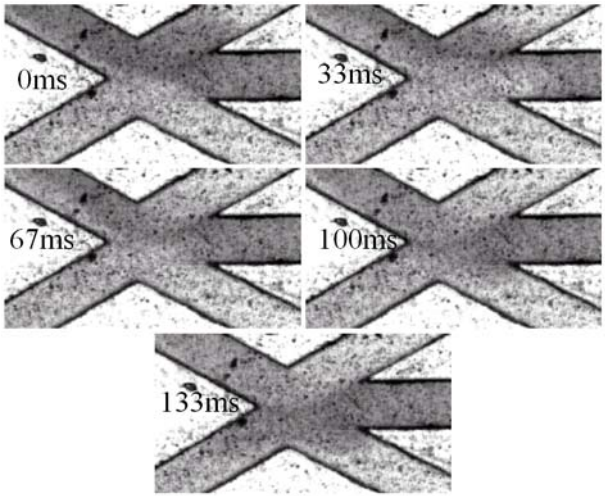

Figure 3: Visualization of the switching time, with ink. Switching time is approximately 133ms, with good agreement to the predicted time of 114ms. Throughput is limited by this time to be approximately 450 cells/min at this velocity. Automation can increase velocity and therefore throughput, discussed in section 5.

The maximum shear stress experienced by the cells corresponds to the largest shear stress in the fluid. The shear stress is defined by [18]

$$\tau = \mu\left(\frac{\partial u_i}{\partial x_j} + \frac{\partial u_j}{\partial x_i}\right) \qquad \textbf{Eq 4}$$

The maximum shear stress was calculated from the computational fluid dynamics simulation results as the matrix 1-norm of the above tensor. We found the maximum stress occurs along the walls, with values of 0.042 Pa. This is on the same order as the analytically-estimated average shear stress [19]:

$$\tau \approx \mu\frac{u}{h/2} \approx 0.02Pa. \qquad \textbf{Eq 5}$$

Typical damaging shear stresses are above 0.4Pa [19]. Therefore this hydrodynamic switching scheme should be safe for cells. This will be tested experimentally using Trypan blue dye in section 4.

3. MANUFACTURING

The chip was manufactured from a 24.9mm x 29.6mm x 11.9mm block of polymethyl methacrylate (PMMA). Channels 127 μm wide x 50 μm deep were surface-machined in an intersecting five-branch configuration using a micro-milling machine (Minimill 3, Minitech Machinery, USA). Figure 4 illustrates the dimensions and major components of the full device. This figure shows the primary chip (A), input reservoir (B), solenoid valves (D), valve-attachment manifold (C), and o-rings (E); details of these components are described further below.

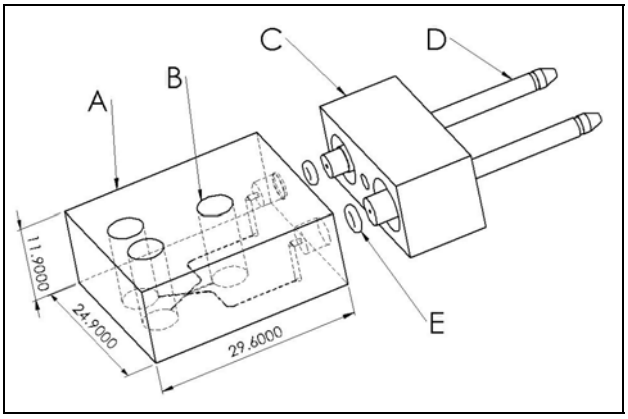

Figure 4. Major components of the cell sorter chip. Dimensions given in mm. See text for further detail. Adhesive tape is applied to the lower chip surface to seal channels

Particles in solution were flowed through a single input branch (Figure 4, B) into either of two output branches. Each of these particle-flow channels terminated in 200ul cylindrical reservoirs so that particle solution could be added and extracted via pipette. As described above, the rate of this particle solution flow was controlled by a difference in fluid level between the input and output reservoirs.

Switching was achieved via alternating the open or closed state of two fast (2kHz operation) solenoid valves (Figure 4, D, from Gyger AG, Switzerland). In this way, a non-stop (particle-free) flow in either of two switching channels diverted the particle solution from the input channel to a specific output channel and reservoir. Transparent adhesive tape was applied to the machined surface of the chip to seal the channels and reservoirs.

The solenoid valves were connected to the chip using a separately-machined PMMA manifold (Figure 4, C); these two components were affixed with a #2-56 socket head cap screw. At the interface, two o-rings (Figure 4, E) sealed the fluid connection between the valves and the chip. A single syringe pump supplied each valve with either isotone buffer or DI water (depending on the sorted particles) via rigid Teflon tubing and a three-way connector.

The valves were actuated using an integrated-circuit controller programmed to supply a peak-and-hold voltage reciprocally to either valve. This signal scheme was necessary in order to maximize the speed of the valves without exceeding their electrical current rating. The controller was constructed to allow for manual operation or triggering from a function generator. The controller additionally required 5V and 12V power supplies.

4. OPERATION AND RESULTS

Experiments were conducted to evaluate (1) the performance of the device as a manual sorter using polymer

spheres and human fibroblasts, and (2) the stress induced by the device on living human fibroblasts after random sorting. The device was then used to separate labeled cells that have been mixed with an unlabeled population of the same cells.

Priming the channels

To prevent clogging by e.g. undesired air bubbles, sorting began with a wetting ('priming') procedure that involved filling all three reservoirs with DI water or filtered isotonic buffer, and then initiating a syringe pump flow of the same solution through the switching channels. A function generator was then used to actuate the valves at high speed (~200Hz) to remove air bubbles attached to the channel walls. During the priming process, the outlet reservoirs were kept filled with liquid.

Sorting polymer beads and human fibroblasts

After wetting, the device performance was evaluated by sorting polymer beads and human fibroblasts. First the input reservoir was filled with an aqueous solution of 11 μm polymer spheres (Duke Scientific, 7510A), at a concentration of 33 particle per μl. Gravity caused the particles to flow from the inlet to the outlet chambers. To demonstrate sorting ability and measure throughput, 101 beads were manually sorted to each output reservoir in an alternating manner over a seven minute span. This results in a measured throughput of approximately 14 cells per minute at velocities of ~1mm/s. Automation and higher velocities can result in higher throughputs, as discussed in section 5. The left side of figure 5 shows (top) an incoming bead, (middle) a bead directed to the top outlet channel, and (bottom) a bead directed to the bottom outlet channel. The inlet reservoir was stained with a small concentration of blue dye to visualize the streaklines of the flow and easily predict where the bead would go.

The same experiment was then performed with trypsinized human fibroblasts. First, the priming procedure was performed with isotonic buffer. Then, cells were trypsinized for 5 minutes, washed, and resuspended in isotonic buffer. A coulter particle counter (Model Z1) was used to determine the concentration of cells (60 cells per μl). After the wetting of the chip, 200μl of the suspended cell solution was added to the input reservoir, and gravity caused the cells to flow between the inlet and outlet reservoirs. The right side of figure 5 shows (top) an incoming bead, (middle) a bead directed to the top outlet channel, and (bottom) a bead directed to the bottom outlet channel. Phase contrast lighting conditions were used to facilitate visualization of the transparent cells, also causing the dark shading on the right side of the images. 30 cells were sorted at velocities of ~0.6mm/s in under 3 minutes, resulting in throughputs of approximately 10 cells per minute. Again this throughput can be increased with automation, discussed in section 5.

Impact of the shear stress on biological cells

While the previous tests showed the capability of the device to precisely sort a particle-laden flow, the device was also tested to evaluate the stress induced on human fibroblasts by the shear stress of the sorting flow. The cells were prepared in the same manner as the previous section and were flowed through the channels from the inlet to the outlet reservoirs. A function generator was used to switch the flow at a rate of 1Hz. After randomly sorting cells for a 20 minute period, 20 μl samples were drawn from each output reservoir and a 40 μl

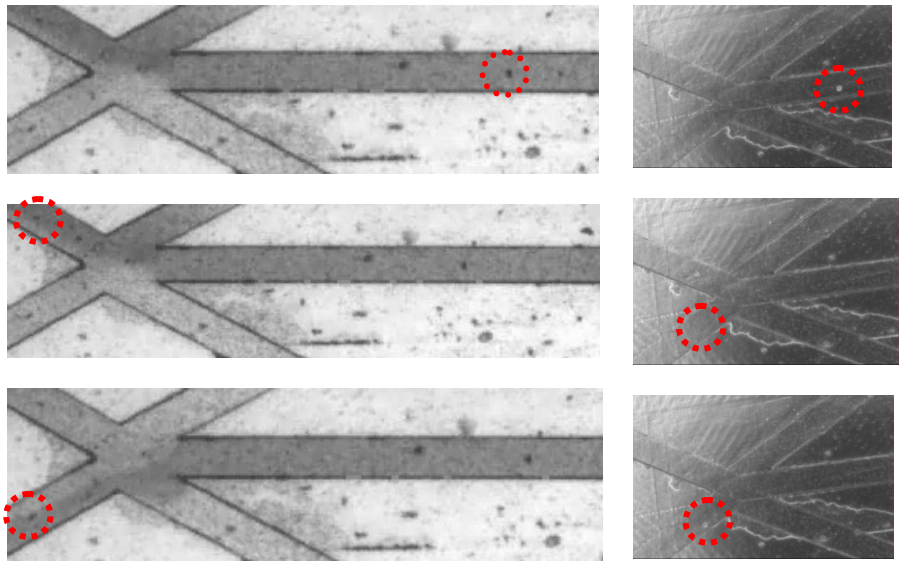

Figure 5: (left) images of sorting polymer beads. The red circles indicate 11 micron polymer beads. The top image shows an incoming bead, the middle image shows the bead directed to the top outlet channel, and the bottom image shows the bead directed to the bottom channel. The bead-laden fluid is lightly dyed with ink to clearly show the direction the bead will take. (right) A similar set of images showing the sorting of trypsinized human fibroblasts. These pictures were taken with phase contrast lighting conditions to facilitate the visualization of the transparent cells, but also causing the dark shading on the right half of the pictures.

control sample was drawn from the input reservoir. Trypan Blue was then used to evaluate the viability of these collected cells under a microscope. The results from this test, shown in Table 1, show a negligible change in the mortality of the sorted cells compared with unsorted cells, indicating an acceptable level of shear stress in the device.

Table 1. Results of cell stress study

	# living cells	# dead cells	% mortality
Input	95	10	10.5
Output	30	4	13.3

Separation of labeled Fibroblasts from unlabeled Fibroblasts

The microfluidic chip described here was then used for separation of cells expressing GFP or stained with vital dyes from non-stained cells in a scenario typical for bystander effect experiments, where fluorescent cells are plated together with non-stained cells and irradiated with a microbeam [3]. An essential step in these types of experiments is the precise separation of the irradiated cells from the non-irradiated cells for subsequent cell analysis.

Two sorting procedures were used during our utilization of the cell sorter: (a) both types of cells are tagged with different colors of fluorescence, or (b) only the irradiated cells are tagged. In the first case, the irradiated cells are labeled with fluorescent nuclear dye (Hoechst 33342) or GFP, and the bystanders are labeled with vital cytoplasmic dye Cell Tracker Orange, and both can be visualized with a double-pass filter. In the second case, only the irradiated nuclei are tagged and sorted from the non-labeled cells. This method ensures that the tagging does not affect the results from the subsequent analysis, and is fully described below.

Normal human fibroblasts (AG01522 cells) expressing GFP or stained with Cell Tracker Green (Molecular probes, Eugene, OR) were plated in ratio of 1:3 with non-stained cells. After 24 hours the cells were trypsinized, washed and resuspended in Isotone to eliminate small particles that are usually present in unfiltered media. A 100 μl suspension of cells with concentration of 20 cells/μl was placed in the inlet reservoir, mixed by pipetting. This initiated a cell flow at a velocity of about 0.5mm/s. Cells reached the sorting zone at a rate of about 1 cell every 10 seconds, and were observed by the operator under the fluorescence microscope by using a combination of filtered fluorescent light (FITC filter) and visual broadband light allowing the user to simultaneously see both fluorescent and non stained cells.

At this stage all cells were driven to the waste chamber by the default state of the controller. Once it was clear that there is a constant flow of cells, the white light was dimmed and cell sorting was performed only under fluorescent light. By pressing a pushbutton switch the flow was directed towards the collection chamber. All fluorescent cells once they appeared in the field of view were directed to the waste chamber by releasing the controller's button. Using a magnification of 4x gives the operator at least 3 seconds to see the fluorescent cells before they reach the cross section of the channels. By operating the chip under only fluorescent light, it is possible to even sort cells with very low levels of fluorescence which might be the case for GFP expressing cells.

It is important to note that successful use of this method ensures that the collection chamber will contain only the non-stained cells of interest, while the waste chamber might contain some non-stained cells, together with the discarded stained cells.

5. AUTOMATION

The above experiments are performed by manually operating the solenoid valves with a pushbutton switch. As a result, the sorting frequency is low (~10 cells/min), but is sufficient for small populations of cells and to prove the concept of this device. The limiting factors to the sorting frequency are the low velocities and the large distance between cells to allow extra time for the operator's reaction reflexes. Automating the detection and sorting would eliminate this requirement for this reaction time and allow much higher throughputs. The maximum theoretical throughput at the current velocity is ~450 cells per minute, limited only by the switching time calculated in section 2 (approx. 130ms). With automated detection, the velocity could increase by an order of magnitude, thereby increasing the throughput by a similar amount. Automation will also lead to decreased operational costs for large populations of cells, as an operator will not be required to perform the sorting.

6. CONCLUSION

A hydrodynamic cell sorter was designed, manufactured and tested to sort cells mechanically under non-damaging shear stress. The cells never stop flowing through the device, reducing the risk of cell adhesion to the surface. The inlet and outlet chambers are easily accessed by pipette, and the main cell flow is driven by gravity. Computational fluid mechanics has been shown to be a useful tool to assist the design and predict device performance. The actuation scheme depends on a syringe pump and two fast microsolenoid valves. The sorter was tested to sort 101 beads in less than 7 minutes, and 30 cells in less than 3 minutes. We show that the maximum throughputs is limited by the flow switching time to ~450 cells per minute. We explain that the flow switching frequency can be increased by increasing the flow velocity, which would be possible using automatic rather than manual cell detection. Finally, operating only under fluorescent light allowed reliable separation of cells even with low fluorescent intensity from non-fluorescent cells.

7. ACKNOWLEDGEMENTS

This work was supported by U19 AI067773, the Center for High-Throughput Minimally Invasive Radiation Biodosimetry, from the NIH/NIAID and NIH grant 5P41EB002033, DOE grant number DE-SC0001634, and the Columbia University department of Mechanical Engineering.

8. REFERENCES

1. Longo, D. and J. Hasty, *Dynamics of single-cell gene expression.* Molecular Systems Biology, 2006. **2**.
2. Lu, J., G. Getz, E.A. Miska, E. Alvarez-Saavedra, J. Lamb, D. Peck, A. Sweet-Cordero, B.L. Ebert, R.H. Mak, A.A. Ferrando, J.R. Downing, T. Jacks, H.R. Horvitz, and T.R. Golub, *MicroRNA expression profiles classify human cancers.* Nature, 2005. **435**(7043): p. 834-838.
3. Hei, T.K., H. Zhou, V.N. Ivanov, M. Hong, H.B. Lieberman, D.J. Brenner, S.A. Amundson, and C.R. Geard, *Mechanism of radiation-induced bystander effects: A unifying model.* Journal of Pharmacy and Pharmacology, 2008. **60**(8): p. 943-950.
4. Berthier, J., Silberzan, P., *Microfluidics for Biotechnology*. 2006, Norwood, MA: Artech House, Inc.
5. Watson, J., *Introduction to Flow Cytometry*. 1991, Cambridge: Cambridge University Press.
6. Fisher, D., Francis, G., Rickwood, D., *Cell Separation: A Practical Approach*. 1998, New York: Oxford University Press.
7. Geens, M., H. Van de Velde, G. De Block, E. Goossens, A. Van Steirteghem, and H. Tournaye, *The efficiency of magnetic-activated cell sorting and fluorescence-activated cell sorting in the decontamination of testicular cell suspensions in cancer patients.* Human reproduction (Oxford, England), 2007. **22**(3): p. 733-742.
8. Andersson, H. and A. Van den Berg, *Microfluidic devices for cellomics: A review.* Sensors and Actuators, B: Chemical, 2003. **92**(3): p. 315-325.
9. Yi, C., C.W. Li, S. Ji, and M. Yang, *Microfluidics technology for manipulation and analysis of biological cells.* Analytica Chimica Acta, 2006. **560**(1-2): p. 1-23.
10. Huh, D., W. Gu, Y. Kamotani, J.B. Grotberg, and S. Takayama, *Microfluidics for flow cytometric analysis of cells and particles.* Physiological Measurement, 2005. **26**(3).
11. Voldman, J., *Engineered systems for the physical manipulation of single cells.* Current Opinion in Biotechnology, 2006. **17**(5): p. 532-537.
12. Takahashi, K., A. Hattori, I. Suzuki, T. Ichiki, and K. Yasuda, *Non-destructive on-chip cell sorting system with real-time microscopic image processing.* Journal of Nanobiotechnology, 2004. **2**.
13. Fu, A.Y., H.P. Chou, C. Spence, F.H. Arnold, and S.R. Quake, *An integrated microfabricated cell sorter.* Analytical Chemistry, 2002. **74**(11): p. 2451-2457.
14. Dittrich, P.S. and P. Schwille, *An Integrated Microfluidic System for Reaction, High-Sensitivity Detection, and Sorting of Fluorescent Cells and Particles.* Analytical Chemistry, 2003. **75**(21): p. 5767-5774.
15. Kruger, J., K. Singh, A. O'Neill, C. Jackson, A. Morrison, and P. O'Brein, *Development of a microfluidic device for fluorescence activated cell sorting.* Journal of Micromechanics and Microengineering, 2002. **12**(4): p. 486-494.
16. White, F., *Fluid Mechanics*. 6th ed. 2008, New York: McGraw-Hill.
17. Bruus, H., *Theoretical Microfluidics*. 2008, New York: Oxford University Press.
18. Aris, R., *Vectors, Tensors, and the Basic Equations of Fluid Mechanics*. 1962, Englewood Cliffs, NJ: Prentice-Hall.
19. Wan, J., W.D. Ristenpart, and H.A. Stone, *Dynamics of shear-induced ATP release from red blood cells.* Proceedings of the National Academy of Sciences of the United States of America, 2008. **105**(43): p. 16432-16437.